Analysis of Effective Axial Diffusion in Branching Networks

William J. Federspiel
Dept. of Biomedical Engineering, Boston University, Boston, MA 02215

Diffusional transport in a network of branching conduits is considered. The branching network is idealized as an ensemble of identical branching segments. Starting with the general species continuity equation, multiscale perturbation analysis is used to derive a one-dimensional, effective transport equation for species concentration. The macrotransport equation contains an effective diffusion coefficient, D^*, which arises naturally from the analysis. D^* can be computed from a local diffusion problem posed on an individual branching segment of the ensemble network. The local relations defining D^* bear clear similarity to their counterparts for transport in spatially periodic porous media. Although this study was originally directed toward describing gas diffusion in the peripheral airspaces of the lung, the results provide insight for other transport processes occurring in branching networks.

Introduction

Many transport processes occur in physical regions which can be characterized by two disparate length scales, a local or "microscopic" scale, and a global or "macroscopic" scale. Solute transport on the microscopic scale is governed unambiguously by the general three-dimensional species continuity equation. In many applications, however, interest lies predominantly, if not exclusively, on solute transport on the macroscopic scale. One simple example is transport in a straight tube, where the local scale is radial tube dimensions and the global scale is the length of the tube. Taylor (1953) demonstrated that global axial transport can be described by a simple one-dimensional macrotransport equation. The macrotransport equation is governed by an effective diffusion or dispersion coefficient, the value of which accounts implicitly for local-scale transport phenomena.

The concepts embodied in Taylor's approach apply equally well to transport in more complex physical regions. The classic paradigm is porous media, where the local scale represents void or particle size, while the global scale represents the ensemble medium. Transport within porous media can be described by a macroscopic transport equation, provided effective transport coefficients are used which account implicitly for the microscale complexities. Accordingly, methods have arisen to determine macrotransport equations and effective transport coefficients for porous media. Most notable are the simple steady-state analyses (Jackson and Coriell, 1968), the moment analysis technique (Brenner, 1980; Shapiro and Brenner, 1988), the volume-averaging technique (Whitaker, 1973; Crapiste et al., 1986), and the method of multiple-scale perturbation (Chang, 1983). These techniques transform microtransport descriptions to valid macrotransport ones and ultimately provide macroscale transport coefficients from computations on a representative unit cell of an assumed periodic porous media.

Not all transport problems with the microscale-macroscale structure fall easily within the periodic porous media paradigm. One example is a dichotomous branching network of conduits. Local scale is defined by the individual branch segments, while global scale is that of the entire network. Macrotransport analyses have been developed for lattice-like networks (often as models of porous media), which are characterized by substantial interconnectedness. The classical approach to lattice-like networks focuses on transport in each conduit branch, with relatively simple mixing laws assumed at bifurcations to connect one branch to another. Examples of such analyses include percolation and effective conduction in resistor networks (Kirkpatrick, 1973), and hydrodynamics in capillary networks (Adler and Brenner, 1984).

This article is concerned with diffusive transport in a dichotomous branching network where bifurcations are not regarded as mere simple connectors. In particular, multiscale perturbation analysis is used to develop a macrotransport theory for diffusion within the network. The branching network

Correspondence concerning this article should be addressed to W. J. Federspiel.

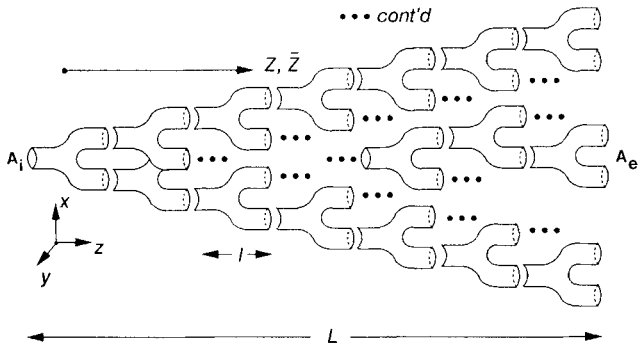

Figure 1. Ensemble branching network.

considered is idealized as an ensemble of identical branching segments; while such a branching network is not spatially periodic, its decomposition into identical branching segments ultimately provides recursion and a "unit cell" formulation for an effective diffusion coefficient. This study was motivated originally by the problem of gas mixing in the peripheral airspace network of the lung (Federspiel and Fredberg, 1988), where convection is relatively minor and branch length is nearly comparable to branch diameter. Nevertheless, the results have useful application for other transport processes, physiological and otherwise, which occur in branching networks.

Theoretical Analysis

Basic geometry and governing equations

Consider the branching network of ducts shown schematically in Figure 1. Location within the network is denoted by the position vector $\vec{r}=(x,y,z)$, with z chosen to represent the axial coordinate along the network. The volume of the branching network is bounded by the wall surface, S_w, of the ducts, and the inlet and exit cross-sectional areas, A_i and A_e, respectively. The branching network is taken to be a repetitive ensemble of identical branching segments, one of which is shown in Figure 2. Accordingly, the branching network exhibits a geometric recursion, but is not spatially periodic in the strict sense (because it "looks" different when viewed in the positive

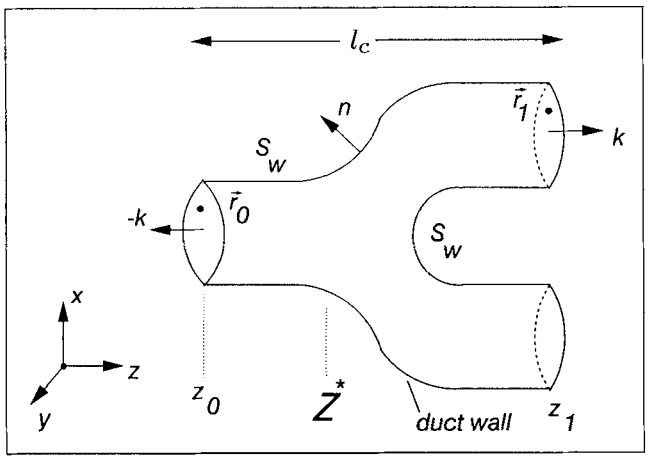

Figure 2. Individual branching segment of the ensemble network.

and negative z directions). The branching network is characterized by a local (microscopic) length, l, corresponding to the scale of the individual branching segment, and a global (macroscopic) length, L, corresponding to the scale of the ensemble network.

We will examine the unsteady diffusional transport of a passive solute with diffusion coefficient, D, within the branching network. The applicable transport equation in dimensionless form is:

$$\epsilon^2 \partial C/\partial t = \nabla^2 C \tag{1}$$

where t is time scaled by the global diffusion time, L^2/D, ∇ is the gradient operator scaled by the local length scale, l, and C is suitably normalized solute concentration. The parameter $\epsilon = l/L$ denotes the ratio of the local to global length scales and is presumed small in the subsequent analysis. The transport formulation is completed with appropriate boundary and initial conditions. The walls of the branching network are regarded as impermeable to the solute so that no flux conditions pertain there:

$$\vec{n} \cdot \nabla C = 0 \quad \vec{r} \in S_w \tag{2}$$

where $\vec{n}$ is the outward unit normal on the wall surface. Also, C satisfies boundary conditions at the ends of the network ($\vec{r} \in A_i$, A_e), and an initial ($t=0$) condition as well, but neither of these need be explicitly specified to proceed with the analysis. The boundary condition at the end of the network ($\vec{r} \in A_e$), however, will be assumed uniform across the network termini.

The macroscale view

On the macroscale, concentration varies predominantly along the axial direction of the network. The pertinent coordinate, therefore, is the global axial coordinate, $\bar{Z}$, scaled by L. Its relation to the locally (l) scaled coordinate, z, is by a simple compression:

$$\bar{Z} = \epsilon z \tag{3}$$

Clearly, the detailed local geometry of the individual branching segment is invisible at the macroscale. Nevertheless, the rapid increase in network cross-sectional area, $A(\bar{Z})$, produced by the branching is a key determinant of species transport. Viewed from the macroscale, the network cross-sectional area appears as a rapidly and continuously varying effective area, $\bar{A}(\bar{Z})$, which preserves the volume characteristics of the network (Figure 3a).

A species mass balance on the macroscale volume element, $\bar{A}(\bar{Z})d\bar{Z}$, shown in Figure 3b provides a macrotransport equation of the form:

$$\partial C/\partial t = D^* \bar{A}(\bar{Z})^{-1} \frac{\partial}{\partial \bar{Z}} \left[\bar{A}(\bar{Z}) \frac{\partial C}{\partial \bar{Z}} \right] \tag{4}$$

where an effective axial diffusion coefficient, D^*, is used to account implicitly for local-scale phenomena, which affect diffusional transport but are lost explicitly at the macroscale. Generally, D^* differs from the molecular diffusion coefficient, D, and must be determined from analyses of local-scale trans-

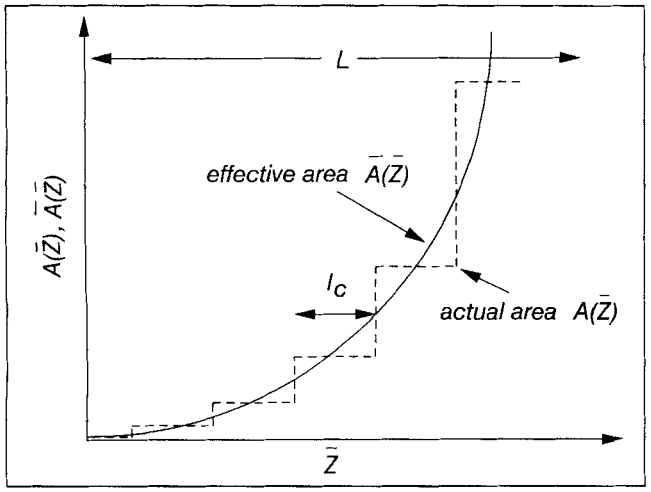

Figure 3a. Schematic showing actual network cross-sectional area vs. effective or macroscopic view of network cross-sectional area.

port. In what follows, we determine D^* by using multiscale perturbation analysis (Nayfeh, 1989) to exploit that the ratio of local to global lengths, ϵ, is presumed small. In this manner the microtransport description, Eqs. 1-2, is transformed to the macrotransport description, Eq. 4.

Multiscale perturbation analysis

A perturbation analysis based on the global coordinate $\bar{Z}$ is ultimately unsuccessful. This is so because the global gradient $\partial C/\partial \bar{Z}$ scales as the inverse of the cumulative cross-sectional area, $\bar{A}(\bar{Z})$, which in turn scales as $\bar{A}(\bar{Z}) \sim 2^{\bar{Z}/\epsilon}$. Hence, $\partial C/\partial \bar{Z}$ is not of $O(1)$, but of $O(2^{-1/\epsilon})$ for fixed $\bar{Z}$ in the limit as $\epsilon \to 0$. Recognizing that the product $\bar{A}(\bar{Z})\partial C/\partial \bar{Z}$ remains $O(1)$ in the limit as $\epsilon \to 0$, we introduce a new global variable, Z, defined by:

$$\partial/\partial Z = \bar{A}(z)\partial/\partial \bar{Z} \tag{5}$$

where a proper scaling of axial derivatives of $\bar{A}$ requires that $\bar{A}$ be regarded as a function of the local axial coordinate z.

Multiscale analysis assumes that C depends independently on the two axial coordinates,

$$C = C(x,y,z,Z,t) = C(\vec{r},Z,t) \tag{6}$$

Accordingly, spatial derivatives in the axial direction must be resolved into local and global contributions:

$$\partial/\partial z \to (\partial/\partial z)_Z + \epsilon \bar{A}(z)^{-1}(\partial/\partial Z)_z \tag{7}$$

where the local coordinate, z, is held fixed during differentiation of the global coordinate, Z, and *vice versa*. For notational convenience we define a function, f, such that $df/dz = f'(z) = \bar{A}^{-1}$, and using Eq. 7, the gradient operator for the multiscale analysis is:

$$\nabla \to \nabla_Z + \vec{k}\epsilon f'(z)\partial/\partial Z \tag{8}$$

where the notation ∇_Z indicates local scale spatial differentiation with Z fixed, that is, $\nabla_Z = (\partial/\partial \vec{r})_Z = (\vec{i}\partial/\partial x + \vec{j}\partial/\partial y + \vec{k}\partial/\partial z)_Z$, with $\vec{i},\vec{j},\vec{k}$ being the usual Cartesian unit vectors.

Equation 8 is introduced into the governing equation, Eq. 1, and an asymptotic solution sought in the limit as $\epsilon \to 0$ with $f'(z)$ and higher derivatives fixed. Accordingly, we expand C in a perturbation series:

$$C = C_0 + \epsilon C_1 + \epsilon^2 C_2 + \ldots \tag{9}$$

and substitute into Eq. 1. Doing so and grouping terms by like powers of ϵ lead to the following sequence of equations governing the concentration fields:

$$L_0 C_0 = 0 \tag{10}$$

$$L_0 C_1 = -L_1 C_0 \tag{11}$$

$$L_0 C_2 = -L_1 C_1 - L_2 C_0 \tag{12}$$

where the indicated operators are defined by:

$$L_0 = \nabla_Z^2 \tag{13}$$

$$L_1 = 2f' \frac{\partial^2}{\partial Z \partial z} + f'' \frac{\partial}{\partial Z} \tag{14}$$

$$L_2 = f'^2 \frac{\partial^2}{\partial Z^2} - \frac{\partial}{\partial t} \tag{15}$$

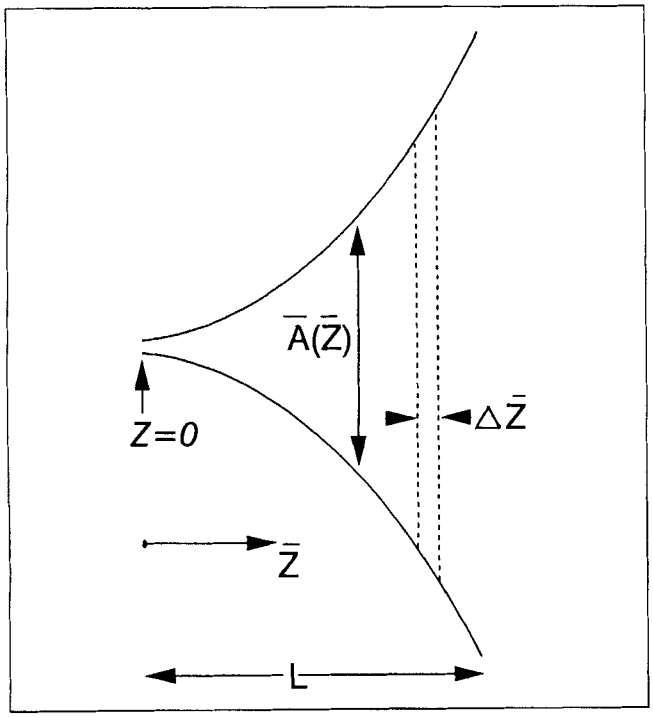

Figure 3b. Macroscale volume element for species conservation balance.

The appropriate boundary conditions on the wall surface follow from substitution of the expansions, Eqs. 8 and 9, into the no-flux boundary condition, Eq. 2. Accordingly,

$$\vec{n}\cdot\nabla_Z C_0 = 0 \tag{16}$$

$$\vec{n}\cdot\nabla_Z C_1 = -\vec{n}\cdot\vec{k}f'(z)\partial C_0/\partial Z \tag{17}$$

$$\vec{n}\cdot\nabla_Z C_2 = -\vec{n}\cdot\vec{k}f'(z)\partial C_1/\partial Z \tag{18}$$

all for $\vec{r}\in S_w$.

The C_0 and C_1 concentration fields

The ∇_Z operator regards Z as fixed. Accordingly, the zero-order concentration field is easily satisfied by an $\vec{r}$-independent solution of the form:

$$C_0 = C_0(Z,t) \tag{19}$$

where $C_0(Z,t)$ can be chosen to satisfy whatever global boundary conditions are of interest at the ends of the network, as well as the initial condition.

Substituting Eq. 19 into Eq. 11 results in the governing equation for the first-order correction to concentration:

$$\nabla_Z^2 C_1 = -f''(z)\partial C_0/\partial Z \tag{20}$$

subject to the wall flux condition:

$$\vec{n}\cdot\nabla_Z C_1 = -\vec{n}\cdot\vec{k}f'(z)\partial C_0/\partial Z \quad \vec{r}\in S_w \tag{21}$$

Equations 20 and 21 suggest a solution of the form:

$$C_1 = \psi(\vec{r})\partial C_0/\partial Z \tag{22}$$

where $\psi(\vec{r})$ satisfies the relations:

$$\nabla_Z^2\psi = -f''(z) \tag{23}$$

$$\vec{n}\cdot\nabla_Z\psi = -\vec{n}\cdot\vec{k}f'(z) \quad \vec{r}\in S_w \tag{24}$$

The wall flux condition on ψ, Eq. 24, will need to be supplemented by appropriate local "periodic" or recursion conditions for $\psi(\vec{r})$ across the individual branching segments. We will derive these in what follows by requiring that the perturbation expansion in C remain uniformly valid in the limit as $\epsilon\to 0$.

The constraint of uniformly valid expressions

Consider some axial location, Z^*, along the network and a local branching segment located there, spanning arbitrarily from $z=z_0$ to $z=z_1$, where $z_1=z_0+l_c$, as shown in Figure 2. In actuality, the local space of the branching network at Z^* is defined by several such branching segments in parallel, the number of which depends on global location along the network. Let $(\vec{r}_0,Z_0)$ represent an arbitrary point on the "parent" face of the local space chosen at Z^*, and let $(\vec{r}_1,Z_1)$ be an equivalent geometric point on the daughter face of the local space. These points are shown for simplicity in Figure 2 on the same branching segment, but clearly $\vec{r}_0$ has equivalent geometric points on its parallel neighbors (not shown) as well. Furthermore, the dichotomy of the network dictates that the number of $\vec{r}_1$ points is twice that of $\vec{r}_0$ points.

The perturbation expansion for C remains uniformly valid when the ratio C_1/C_0 is the same at equivalent points across the branching segments, or

$$(C_1/C_0)_{\vec{r}_1,Z_1} = (C_1/C_0)_{\vec{r}_0,Z_0} \tag{25}$$

That this is so can be appreciated from the following arguments. A fixed global position, Z, is of $O(1/\epsilon)$ number of bifurcations from the first generation in the network. If $(C_1/C_0)_{\vec{r}_1}=\kappa(C_1/C_0)_{\vec{r}_0}$, where κ is any constant, and if C_1/C_0 is of $O(1)$ at the first generation, then over $1/\epsilon$ generations, C_1/C_0 at Z would be of $O(\kappa^{1/\epsilon})$. A uniformly valid expansion, however, requires C_1/C_0 to remain $O(1)$ for fixed Z as $\epsilon\to 0$. Thus, κ must be equal to unity as indicated by Eq. 25.

We proceed by translating the recursion relation for C_1 to one for ψ. The transforms, Eqs. 3 and 5, can be used to show that $Z=\epsilon f(z)$. Thus, $Z_1=Z_0+\epsilon\Delta f$, where $\Delta f=f(z_1)-f(z_0)$, and we can use Taylor expansions in Z to relate arguments at Z_1 to those at Z_0. Doing so yields $C_0(\vec{r}_1,Z_1)=C_0(Z_1)$ $=C_0(Z_0)+\epsilon\Delta f\partial C_0/\partial Z_{Z_0}$, and $C_1(\vec{r}_1,Z_1)=\psi(\vec{r}_1)\partial C_0/\partial Z_{Z_1}$ $=\psi(\vec{r}_1)[\partial C_0/\partial Z_{Z_0}+\epsilon\Delta f\partial^2 C_0/\partial Z_{Z_0}^2]$. Substituting these expansions into Eq. 25 and letting $\epsilon\to 0$ results in the recursion relation:

$$\psi_1(\vec{r}_1)=\psi(\vec{r}_0) \tag{26}$$

The expansion for the concentration gradient (hence flux) must also remain uniformly valid. Accordingly, we impose a similar constraint on the first order correction to ∇C:

$$(\nabla C_1/\nabla C_0)_{\vec{r}_1,Z_1} = (\nabla C_1/\nabla C_0)_{\vec{r}_0,Z_0} \tag{27}$$

Using the multiscale gradient operator, Eq. 8, and the solutions for C_0 and C_1 solutions, Eqs. 19 and 22, results in ∇C_0 $=\epsilon\vec{k}f'(z)\partial C_0/\partial Z$, and $\nabla C_1=\nabla_Z\psi\partial C_0/\partial Z+\epsilon\vec{k}f'(z)\psi\partial^2 C_0/\partial Z^2$. Proceeding, we use Taylor expansions as before to relate arguments evaluated at Z_1 to those at Z_0. Doing so and taking the limit as $\epsilon\to 0$, with use of $\psi(\vec{r}_1)=\psi(\vec{r}_0)$, result in the recursion relation:

$$(\nabla_Z\psi)_{\vec{r}_1}=\frac{f'(z_0+l_c)}{f'(z_0)}(\nabla_Z\psi)_{\vec{r}_0}=\frac{1}{2}(\nabla_Z\psi)_{\vec{r}_0} \tag{28}$$

where the rightmost equality follows from noting that $f'(z)$ $=\overline{A}(z)^{-1}$, and in the network considered $\overline{A}(z_0+l_c)$ $=2\overline{A}(z_0)$.

The recursion relation for $\nabla_Z\psi$ leads to a useful and easily understood integral constraint for C_1. Equation 28 indicates that the total local flux of C_1 at the parent face of the branching segments at Z^* balances that at the daughter face. This is so because $C_1=\psi(\vec{r})\partial C_0/\partial Z$ and daughter face area is twice that of the parent face. Accordingly, the local production of C_1 dictated by the source term in Eq. 20 balances the loss of C_1 from the flux at the wall, Eq. 21. If this were not so, then viewed globally the branching segments (that is, the local space) would represent a point source (or sink) for C_1, and C_1 would be a more secular term globally than C_0, which is governed

locally by a homogeneous problem. Hence, a necessary condition for a uniformly valid C_1 perturbation term is:

$$\int_{V_c} \nabla_Z^2 C_1 dV = \int_{S_w} \vec{n} \cdot \nabla_Z C_1 dS \tag{29}$$

where V_c is the local space volume of the branching network at Z^*, and S_w is the combined wall surface of the branching segments located there.

Our choice of the transformed global variable, $Z = \epsilon f(z)$, leaves the integral constraint for C_1 automatically satisfied, as is easily demonstrated. Eq. 29 can be recast as:

$$\int_{V_c} -f''(z)\partial C_0/\partial Z dV = \int_{S_w} -\vec{n} \cdot \vec{k} f'(z)\partial C_0/\partial Z dS \tag{30}$$

by using Eqs. 20 and 21. The global gradient $\partial C_0/\partial Z$ is constant to $O(\epsilon)$ over the integration limits and can be eliminated. Thus, the left side is equivalent to $\int_{V_c} -\nabla \cdot \vec{k} f'(z) dV$, which can be expressed as the *closed* surface integral $\oint_{S_c} -\vec{n} \cdot \vec{k} f'(z) dS$ using the divergence theorem. The wall surface contribution of the closed surface integration will cancel the right side of Eq. 30, leaving only contributions from the parent and daughter cross-sectional faces. Upon noting the orientation of the outward normals on these faces, the constraint takes the form:

$$f'(z_0 + l_c) A(z_0 + l_c) = f'(z_0) A(z_0) \tag{31}$$

where $A(z)$ is the total cross-sectional area of the network at z. Since $f'(z) = \overline{A}^{-1}$ and $\overline{A}(z_0 + l_c)/\overline{A}(z_0) = A(z_0 + l_c)/A(z_0)$, it follows that Eq. 31 is satisfied. Clearly, use of the global variable, $\overline{Z} = \epsilon z$, would have been unsuccessful, as $f'(z) = 1$ for this choice and hence Eq. 31 and the integral constraint is not satisfiable.

The C_2 concentration field

Substituting the assumed forms of the C_0 and C_1 solutions, Eqs. 19 and 22, into the governing equation and boundary condition for C_2 (Eqs. 12 and 18, respectively) yields:

$$\nabla_Z^2 C_2 = (-2f'\psi_z - f''\psi - f'^2)\partial^2 C_0/\partial Z^2 + \partial C_0/\partial t \tag{32}$$

and the wall flux condition:

$$\vec{n} \cdot \nabla_Z C_2 = -\vec{n} \cdot \vec{k} f' \psi \partial^2 C_0/\partial Z^2 \quad \vec{r} \in S_w \tag{33}$$

where $\psi_z = \partial\psi/\partial z$. It will not be necessary to solve for C_2 directly. Instead it will suffice to require that C_2 remain a uniformly valid perturbation term, as was done for C_1. Accordingly, we will subject C_2 to the integral constraint, Eq. 29, applied to the local space of the branching segments at Z^*. Doing so and using Eqs. 32 and 33 leads to the requirement that:

$$\int_{V_c} [(-2f'\psi_z - f''\psi - f'^2)\partial^2 C_0/\partial Z^2 + \partial C_0/\partial t] dV = \int_{S_w} -\vec{n} \cdot \vec{k} f' \psi \partial^2 C_0/\partial Z^2 dS \tag{34}$$

We can simplify Eq. 34 by converting the surface integral into a volume integral. In what follows, we make implicit use that $\partial^2 C_0/\partial Z^2$ is constant to $O(\epsilon)$ on the scale of the individual branching segments and need not be considered explicitly in evaluating integrals. Since $-\vec{n} \cdot \vec{k} f' = \vec{n} \cdot \nabla_Z \psi$ on S_w (Eq. 24), the local portion of the surface integrand in Eq. 34 can be written as $\vec{n} \cdot \psi \nabla_Z \psi$. The closed surface, S_c, bounding V_c is composed of the wall surface, S_w, and the areas of the parent and daughter faces, $A(z_0)$ and $A(z_0 + l_c)$. Hence,

$$\oint_{S_c} \vec{n} \cdot \psi \nabla_Z \psi dS = \int_{S_w} \vec{n} \cdot \psi \nabla_Z \psi dS + \int_{A(z_0 + l_c)} \vec{k} \cdot \psi \nabla_Z \psi dS - \int_{A(z_0)} \vec{k} \cdot \psi \nabla_Z \psi dS \tag{35}$$

where the latter two integrals follow upon noting the orientation of $\vec{n}$ on the parent and daughter faces of the branching segments. The recursion relations for ψ and $\nabla_Z \psi$, in conjunction with the doubling in area from parent to daughter face, dictate that the last two integrals cancel each other. Accordingly, the wall surface integral in Eq. 34 can be written as the closed surface integral:

$$\int_{S_w} -\vec{n} \cdot \vec{k} f' \psi dS = \oint_{S_c} \vec{n} \cdot \psi \nabla_Z \psi dS \tag{36}$$

Using the divergence theorem on the right side of Eq. 36, expanding the resulting $\nabla_Z \cdot \psi \nabla_Z \psi$ as $\psi \nabla_Z^2 \psi + \nabla_Z \psi \cdot \nabla_Z \psi$, and recalling from Eq. 23 that $\nabla_Z^2 \psi = -f''$, the surface integral becomes:

$$\int_{S_w} -\vec{n} \cdot \vec{k} f' \psi \partial^2 C_0/\partial Z^2 dS = \int_{V_c} (-f''\psi + \nabla_Z \psi \cdot \nabla_Z \psi)\partial^2 C_0/\partial Z^2 dV \tag{37}$$

Substituting Eq. 37 into Eq. 34, introducing a new local function, $\Phi(\vec{r}) = \psi(\vec{r}) + f(z)$, and combining terms gives us the governing equation:

$$\partial C_0/\partial t = K^* \partial^2 C_0/\partial Z^2 \tag{38}$$

where

$$K^* = V_c^{-1} \int_{V_c} \nabla_Z \Phi \cdot \nabla_Z \Phi dV \tag{39}$$

The governing problem for $\Phi(\vec{r})$ follows from that for ψ upon substituting $\psi(\vec{r}) = \Phi(\vec{r}) - f(z)$ into Eqs. 23, 24, 26 and 28. Thus, Φ satisfies:

$$\nabla_Z^2 \Phi = 0 \tag{40}$$

$$\vec{n} \cdot \nabla_Z \Phi = 0 \quad \vec{r} \in S_w \tag{41}$$

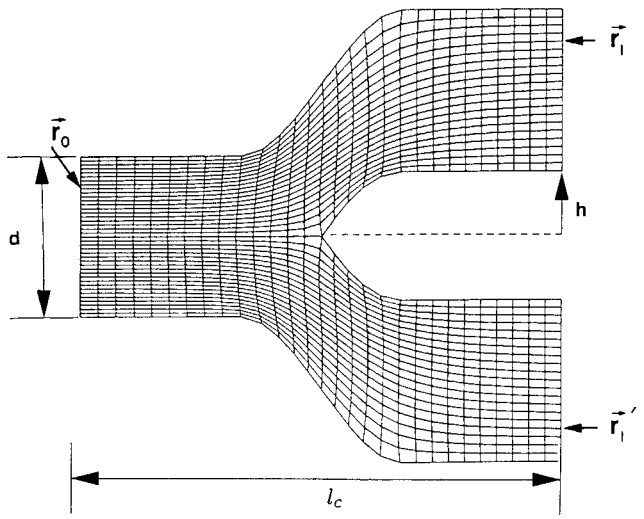

Figure 4. Numerically generated curvilinear grid and geometric parameters for model planar branching segment.

and the recursion relations:

$$\Phi(\vec{r}_1) - \Phi(\vec{r}_0) = f(z_0 + l_c) - f(z_0) \tag{42}$$

$$\vec{k} \cdot \nabla_Z \Phi(\vec{r}_1) = \frac{1}{2} \vec{k} \cdot \nabla_Z \Phi(\vec{r}_0) \tag{43}$$

The effective transport equation

A macrotransport equation based on the physical global coordinate, $\overline{Z}$, is more useful than one based on the transformed global coordinate, Z. Accordingly, we can recast Eq. 38 using the transform definition, Eq. 5:

$$\partial C_0/\partial t = K^* \overline{A}(\overline{Z}^*) \frac{\partial}{\partial \overline{Z}} \left[\overline{A}(\overline{Z}^*) \frac{\partial C_0}{\partial \overline{Z}} \right] \tag{44}$$

where the area, $\overline{A}(\overline{Z})$, is evaluated at the global location of the branching segments, $\overline{Z} = \overline{Z}^*$. The coefficient K^*, however, depends on the axial position of the branching segment through the recursion condition, Eq. 42, but we eliminate this dependence by recasting the problem as follows.

The choice of the branching segments (local space) at axial position $z^*, \overline{Z}^*$ has thus far been arbitrary. We will select instead the branching segment at z^* which satisfies:

$$f(z_0 + l_c) - f(z_0) = f'(z^*) l_c = \overline{A}^{-1}(\overline{Z}^*) l_c \tag{45}$$

Provided $z_0 \le z^* \le z_0 + l_c$, we are guaranteed that the requisite selection can be made. Proceeding, we introduce a scaled local function, $B(\vec{r}) = \Phi(\vec{r})/f'(z^*) = \overline{A}(\overline{Z}^*)\Phi(\vec{r})$ and substitute into Eqs. 40 through 43 to derive the governing problem for the B field:

$$\nabla_Z^2 B = 0 \tag{46}$$

$$\vec{n} \cdot \nabla_Z B = 0 \quad \vec{r} \in S_w \tag{47}$$

$$B(\vec{r}_1) - B(\vec{r}_0) = l_c \tag{48}$$

$$\vec{k} \cdot \nabla_Z B(\vec{r}_1) = \frac{1}{2} \vec{k} \cdot \nabla_Z B(\vec{r}_0) \tag{49}$$

where the recursion condition for B is simplified using Eq. 45, and where $\overline{A}(\overline{Z}^*)$ is recognized as a constant with respect to the local Φ and B problem.

The final form of the solute macrotransport equation follows from introducing the B field into Eqs. 39 and 44:

$$\partial C_0/\partial t = D^* \overline{A}(\overline{Z})^{-1} \frac{\partial}{\partial \overline{Z}} \left[\overline{A}(\overline{Z}) \frac{\partial C_0}{\partial \overline{Z}} \right] \tag{50}$$

where D^* is an effective axial diffusion coefficient whose value depends solely on the B field according to:

$$D^* = D V_c^{-1} \int_{V_c} \nabla_Z B \cdot \nabla_Z B \, dV \tag{51}$$

(The molecular diffusion coefficient, D, appears in the definition if the macrotransport equation is regarded in dimensional form.) Although derived specifically at $\overline{Z} = \overline{Z}^*$, the macrotransport equation applies to all $\overline{Z}$, as the choice of $\overline{Z}^*$ was arbitrary.

Application of Theory

Effective diffusion coefficients were evaluated for symmetric two-dimensional branching segments, as shown in Figure 4. Numerically generated curvilinear grids were produced which "fit" the bifurcating segments (see Figure 4). These curvilinear grids were generated using elliptic grid generation techniques as described in Thompson et al. (1985). Subsequently, the equations and boundary conditions governing the B field (Eqs. 46–49) were transformed to the curvilinear coordinate system and discretized using second-order finite difference derivative approximations. Application of the resulting finite difference expressions to each grid point provided a system of coupled algebraic equations, which were solved using successive overrelaxation iterative techniques. Once the discretized B field was obtained, D^* values followed from numerical integration of the finite difference form of Eq. 51.

The choice of a simple symmetric bifurcating segment allowed the B field problem and associated recursion relations to be applied on a single bifurcating segment, as follows. We will refer to each branch arising from a bifurcation as either a left branch (upper branch in Figures 2 and 4) or a right branch (lower branch in Figures 2 and 4). If we assume for the sake of argument that the parent branch in Figure 4 is itself a left branch (of the preceding bifurcation not shown) and label an arbitrary point $\vec{r}_0$ there, then we can immediately identify its equivalent geometric point $\vec{r}_1$ on the left daughter branch, as indicated in Figure 4. We then invoke symmetry arguments to locate another equivalent point, $\vec{r}_1'$, on the right branch as shown in Figure 4. These symmetry arguments are possible not only because the bifurcating segments are geometrically symmetric, but also because the boundary conditions at the ends of the network (at A_i and A_e) are assumed uniform, independent of x,y. If the parent branch in Figure 4 were a right branch of the preceding bifurcation, then our

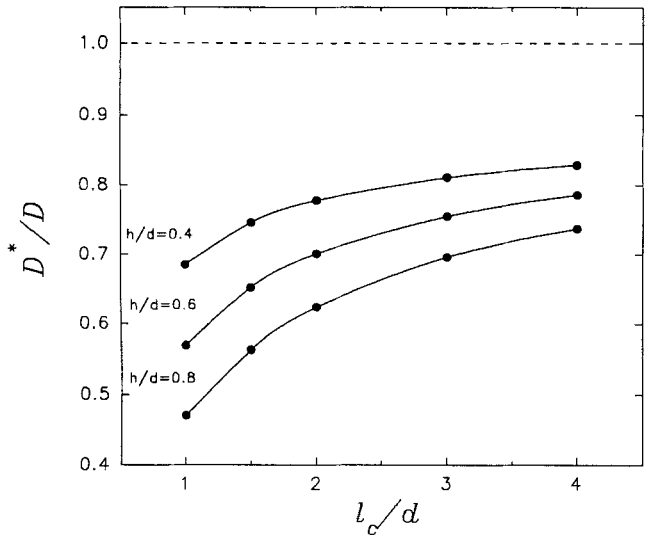

Figure 5. Effective axial diffusion coefficients, D^*, in model branching segment.

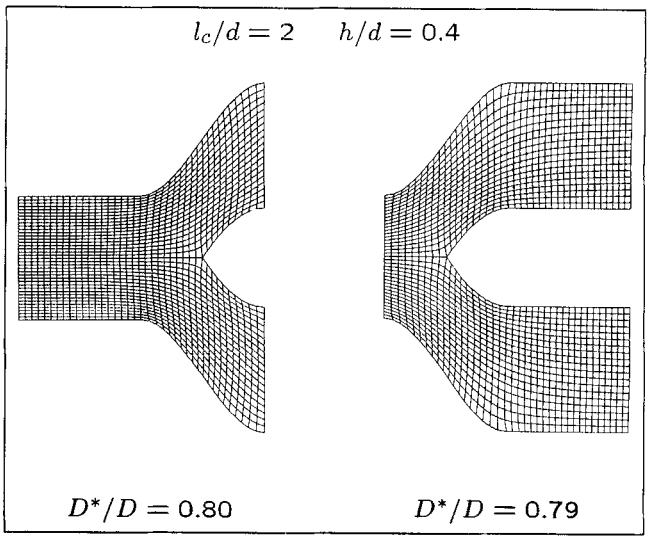

Figure 7. Invariance of D^* with respect to choice of branching segment for fixed geometric parameters.

arguments would still apply in the "mirror" sense to those described above. Furthermore, the B field would be a "mirror" image to that for a left parent branch, and the D^* values computed would be the same for either scenario. The computations presented here were done assuming the parent branch to be a left branch.

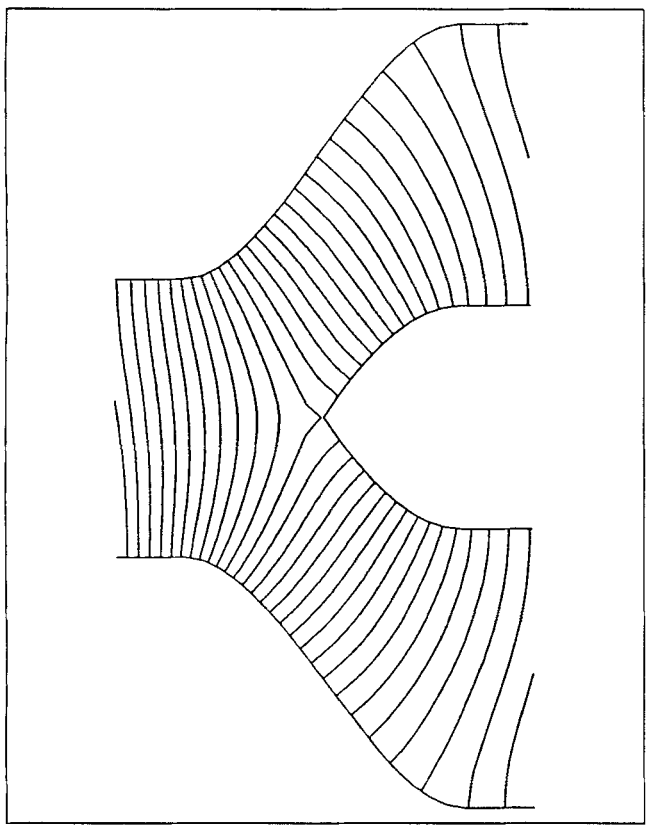

Figure 6. Example of B field contours in the model branching segment.

Computed effective diffusion coefficients are shown in Figure 5. D^* values, normalized by the molecular diffusion coefficient, D, are displayed vs. normalized branch segment length, l_c/d. Results are shown for several values of normalized daughter branch deflection, h/d, a measure of the tortuosity of the branching. The effective diffusion coefficient is reduced relative to the molecular diffusion coefficient. The degree of the reduction depends on the local morphology of the bifurcation segment as measured by the l_c/d and h/d parameters. Shown in Figure 6 are contours of the B field computed for one specific geometry ($l_c/d = 1.5$ and $h/d = 0.4$).

The computed D^* values were insensitive to how the individual branch segment was selected for a fixed set of geometric parameters. As example, Figure 7 displays two markedly different representations of branching segments chosen in a network characterized by $l_c/d = 2$ and $h/d = 0.4$. The respective D^*/D values computed were 0.80 and 0.79. This difference is within the range of variation of D^* resulting from use of different grids for the same branching segment.

Discussion

Diffusive transport in branching networks composed of identical branching segments can be described by a macrotransport equation. The macrotransport equation is governed by an effective axial diffusion coefficient, D^*, whose value depends solely on local diffusion and geometry at the scale of the individual branching segment. In this regard, diffusive transport in these branching networks appears analogous to that in spatially periodic porous media (Brenner, 1980; Chang, 1983; Crapiste et al., 1986; Shapiro and Brenner, 1988). Naturally, the macrotransport equation, which evolves for branching networks, accounts for the increase in the cross-sectional area along the network. This is a dominant feature for species transport in branching networks, but is absent in spatially periodic media.

Though the macrotransport equation for branching networks differs expectedly from that for porous media, the ef-

fective diffusion coefficient, D^*, bears a striking resemblance to that for porous media. In particular, the local diffusional B field problem, which provides the integral relation for D^*, is essentially identical to its porous media counterpart for diffusional transport (cf. Brenner, 1980). One notable difference occurs in the recursion (jump) condition for the B field flux (Eq. 49), which in branching networks accounts for the area increase across the branching segment. The similarity to porous media theory arises despite the fundamental differences between the multiscale perturbation analysis used here and the moment analysis used for spatially periodic porous media. Indeed, the moment analysis technique as used for spatially periodic porous media cannot be easily applied to the branching network problem.

The analysis presented implicitly assumes that the boundary condition imposed at the ends of the ensemble network is uniform across termini. Thus, on the time scale of the global diffusion time (L^2/D) as used here, the local concentration field throughout the network has adjusted to the uniformly applied global terminal conditions. By implication solute concentration *on the macroscale* will vary primarily along the axial direction of the network and will not exhibit global variations laterally (that is, across parallel branching segments). Accordingly, the analysis presented here introduces a single global coordinate (axial coordinate) and presumes predominant macroconcentration dependence along that coordinate. One possible extension of the analysis would be to develop a three-dimensional macrotransport description which allows for global variations in terminal conditions and/or allows for time scales less than the overall global diffusion time (though still greater than *local* diffusion time).

In the moment analysis for spatially periodic media, D^* arises formally from the rate at which the variance of tracer position increases with time. As such, it bears the phenomenological significance of a dispersion coefficient in a stochastic process. Here, we refer to D^* as an "effective diffusion coefficient" because it arises as a coefficient in a one-dimensional effective transport equation. Whether the nomen "dispersion coefficient" can be ascribed to our D^* is not clear. The moment analysis for spatially periodic media appears most suited for answering questions of this nature, but first needs to be extended to the branching network problem. In this regard, the analysis presented here may prove to be a useful guide.

Acknowledgment

This work was supported by Grant HL-33009 from the National Heart, Lung, and Blood Institute. I am grateful to Kerry A. Corrigan for assistance in the numerical computations.

Notation

$\underline{A}$ = actual total cross-sectional area of network at z
$\overline{A}$ = macroscopic view of cross-sectional area of network
B = local field defining effective diffusion coefficient
C = species concentration
C_i = ith concentration perturbation
d = diameter of branch duct
D = molecular diffusion coefficient
D^* = effective diffusion or dispersion coefficient
f = local function defined by $f'=\overline{A}^{-1}$
h = deflection of daughter branch in model branch segments
$\vec{i}$ = unit vector in x direction
$\vec{j}$ = unit vector in y direction
$\vec{k}$ = unit vector in z direction
K^* = macrotransport coefficient
l = local-scale characteristic dimension
l_c = axial length of individual branch segment
L = global-scale characteristic dimension
L_i = linear operator defining C_i
$\vec{n}$ = unit normal vector on a surface
O = perturbation symbol expressing order of
$\vec{r}$ = local-scale position vector
S_w = wall surface area
t = time
V_c = local space volume of branching segments at Z^*
x = local-scaled rectangular coordinate
y = local-scaled rectangular coordinate
z = local-scaled axial coordinate
Z = global-scaled and transformed axial coordinate
$\overline{Z}$ = global-scaled physical axial coordinate

Greek letters

ϵ = perturbation quantity given by l/L
ψ = local-scale field determining C_1
Φ = local-scale field given by $\psi+f$
∇ = gradient operator

Subscripts/superscripts

0 = point on parent face of local branching segment
1 = equivalent point on daughter face
c = entire branching segment
e = end of network
i = inlet to network
w = pertaining to wall of branching segment
* = denoting position of selected branching segment

Literature Cited

Adler, P. M., and H. Brenner, "Transport Processes in Spatially Periodic Capillary Networks: I. Geometrical Description and Linear Flow Hydrodynamics," *Physico Chem. Hydrodyn.*, **5**(3/4), 245 (1984).

Brenner, H., "Dispersion Resulting from Flow Through Spatially Periodic Porous Medium," *Phil. Trans. R. Soc. Lond.*, **297**, 81 (1980).

Chang, H.-C., "Effective Diffusion and Conduction in Two-Phase Media: a Unified Approach," *AIChE J.*, **29**(5), 846 (1983).

Crapiste, G. H., E. Rotstein, and S. A. Whitaker, "A General Closure Scheme for the Method of Volume Averaging," *Chem. Eng. Sci.*, **41**(2), 227 (1986).

Federspiel, W. J., and J. J. Fredberg, "Axial Dispersion in Respiratory Bronchioles and Alveolar Ducts," *J. Appl. Physiol.*, **64**(6), 2614 (1988).

Kirkpatrick, S., "Percolation and Conduction," *Revs. Mod. Phys.*, **45**(4), 574 (1973).

Jackson, J. L., and S. R. Coriell, "Transport Coefficients of Composite Materials," *J. Appl. Phys.*, **39**(3), 2349 (1968).

Nayfeh, A. H., *Perturbation Methods*, p. 228, Wiley, New York (1989).

Shapiro, M., and H. Brenner, "Dispersion of a Chemically Reactive Solute in a Spatially Periodic Model of a Porous Medium," *Chem. Eng. Sci.*, **43**(3), 551 (1988).

Taylor, G., "Dispersion of Soluble Matter in Solvent Flowing Slowly Through a Tube," *Proc. R. Soc. Lond. (A)*, **219**, 186 (1953).

Thompson, J. F., Z. U. A. Warsi, and C. W. Mastin, *Numerical Grid Generation*, North-Holland, New York (1985).

Whitaker, S., "The Transport Equations for Multi-Phase Systems," *Chem. Eng. Sci.*, **28**, 139 (1973).

Manuscript received Aug. 14, 1991, and revision received May 28, 1992.